JACS
JOURNAL OF THE AMERICAN CHEMICAL SOCIETY

Communication

pubs.acs.org/JACS

Identification of a Foldaxane Kinetic Byproduct during Guest-Induced Single to Double Helix Conversion

Quan Gan,[†,‡] Yann Ferrand,[†,‡] Nagula Chandramouli,[†,‡] Brice Kauffmann,[§,∥,⊥] Christophe Aube,[#] Didier Dubreuil,[#] and Ivan Huc*[,†,‡]

[†]Université de Bordeaux, CBMN (UMR 5248), Institut Européen de Chimie Biologie, 2 rue Escarpit, 33607 Pessac, France

[‡]CNRS, CBMN (UMR 5248), Institut Européen de Chimie Biologie, 2 rue Escarpit, 33607 Pessac, France

[§]Université de Bordeaux, Institut Européen de Chimie Biologie (UMS 3033/US 001), F-33600 Pessac, France

[∥]CNRS, Institut Européen de Chimie Biologie (UMS 3033), F-33600 Pessac, France

[⊥]INSERM, Institut Européen de Chimie Biologie (US 001), F-33600 Pessac, France

[#]Université de Nantes, CNRS, Chimie et Interdisciplinarité: Synthèse, Analyse, Modélisation (CEISAM), UMR 6230, Faculté des Sciences et des Techniques, 2 rue de la Houssinière, BP 92208, 44322 Nantes Cedex 3, France

Supporting Information

ABSTRACT: An aromatic oligoamide sequence was designed and synthesized to fold in a single helix having a large cavity and to behave as a host for a dumbbell-shaped guest derived from tartaric acid. NMR, molecular modeling, and circular dichroism (CD) evidence demonstrated the rapid formation of this 1:1 host–guest complex and induction of the helix handedness of the host by the guest. This complex was found to be a long-lived kinetic supramolecular byproduct, as it slowly transformed into a 2:2 host–guest complex with two guest molecules bound at the extremities of a double helix formed by the host, as shown by NMR and CD spectroscopy and a solid-state structure. The guest also induced the handedness of the double helical host, but with an opposite bias. The chiroptical properties of the system were thus found to revert with time as the 1:1 complex formed first, followed by the 2:2 complex.

The comprehension of kinetically controlled reaction steps in supramolecular events is crucial for the construction of out-of-equilibrium artificial ordered aggregates,[1] complex self-assemblies,[2] and sophisticated molecular machines[3] that would resemble their biological counterparts. In the present study, we show that mixing a helical host and a chiral guest results in the formation of a transient supramolecular species that gives rise to a temporary chiroptical signature opposite to that observed at equilibrium. Specifically, a tartaric acid-derived guest rapidly interacts with a single helical aromatic oligoamide foldamer that can wrap around it to form a 1:1 host–guest complex with a preferred handedness. This complex then progressively transforms into a thermodynamically more favorable 2:2 architecture composed of two guests and a double helix and having a handedness opposite to that of the 1:1 complex. The same guest is thus able to induce *P* or *M* helicity depending on whether it interacts with a single or a double helix. These results represent a striking illustration of the multiple processes that compete and take place on different time scales in supramolecular reaction sequences.

We recently introduced the helical aromatic oligoamide foldamer molecular capsule **1**, which can bind tartaric acid diastereoselectively (Chart 1).[4] Its design is based on amino acid units coding for a large helix cavity in the center of the sequence and a narrow helix diameter at the ends, thus creating a binding site completely surrounded by the helix backbone. In a subsequent work, we showed that multiturn single- or double-helical oligoamide foldamers possessing open cavities can wind around urethane dumbbell guests to form thermodynamically stable complexes in which the two bulky stoppers of the guest protrude from the two ends of the helix cavity in a pseudorotaxane-like geometry (Figure 1, top right).[3b,5,6] These complexes were termed foldaxanes.[5] We envisioned that a combination of these two concepts may allow the creation of foldaxanes using dumbbell guests such as **3** derived from tartaric acid.

Chart 1. Formulas of Oligomers 1 and 2 and Dumbbell Guest 3[a]

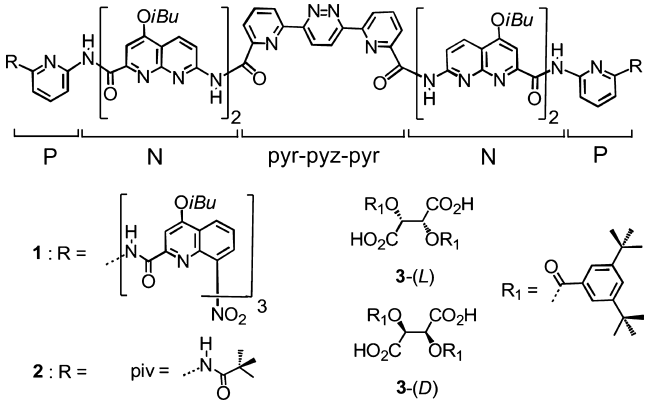

[a]A letter code is used for the abbreviations of the oligomer subunits.

Received: July 2, 2012

   dx.doi.org/10.1021/ja3064364 | J. Am. Chem. Soc. XXXX, XXX, XXX–XXX

Oligomer **2** was designed for this purpose. Its sequence is a shortened version of **1** in which the terminal quinoline units that would close the cavity have been replaced by pivaloyl (piv) groups. The helix of **2** was thus expected to possess an open cavity. Naphthyridine (**N**) units were kept in the design because they are directly involved in intermolecular hydrogen bonding to tartaric acid.[4] The synthesis of **2** involves the piv-**PN**$_2$-Boc building block, which after Boc cleavage was coupled twice to the acids of the central pyridine−pyridazine−pyridine (**pyr−pyz−pyr**) unit [see the Supporting Information (SI)]. The two optically pure enantiomers **3**-(D) and **3**-(L) were prepared by coupling of 3,5-di-*tert*-butylbenzoyl chloride to D- and L-dibenzyl tartrate, respectively, followed by Pd/C-catalyzed hydrogenolysis of the benzyl groups.[7]

A preliminary investigation of the behavior of **2** in solution revealed that like many other aromatic amide sequences,[8] its single-helical conformation is in equilibrium with a double-helical species (Figure 1 left). This is reflected by, for example,

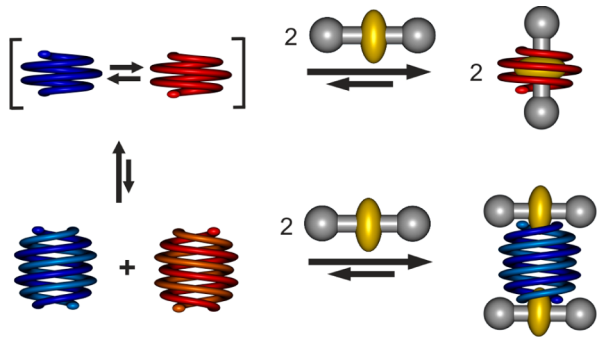

Figure 1. (left) Equilibrium between oligomer **2** as *P* (blue) and *M* (red) single helices and *P* and *M* double helices. (top) Equilibrium between oligomer **2** as *P* and *M* single helices and (*M*)-**2**⊃**3**-(L). (bottom) Equilibrium between oligomer **2** as *P* and *M* double helices and a 2:2 complex between $[(P)\text{-}\mathbf{2}]_2$ as a double helix and two **3**-(L) molecules. It should be noted that the *P* and *M* single helices are at equilibrium, whereas the *P* and *M* double helices are not unless they first dissociate into single helices.

two sets of signals in the ^{1}H NMR spectrum that are assigned to the monomer and the dimer, the proportions of which vary with concentration. A ^{1}H diffusion-ordered spectroscopy (DOSY) measurement on a 2 mM solution of **2** at 293 K (Figure S2 in the SI) showed two distinct diffusion coefficients for **2** and its double helix $(\mathbf{2})_2$, which were calculated to be 7.38×10^{-10} and 6.44×10^{-10} m^2 s^{-1}, respectively. However, unlike for other aromatic amide double helices,[8] we found that the NMR signals of the double helix also varied with concentration ($\Delta\delta$ up to 0.2 ppm), indicating another aggregation phenomenon that takes place rapidly on the NMR time scale. Self-aggregation of the double helices themselves due to the aromatic and hydrogen bonding groups present at their termini could explain these chemical shift variations. This resulted in a bias of the single helix ⇄ double helix equilibrium, which shifted in favor of the double helix at high concentration. For example, the apparent dimerization constants were measured to be 420 M^{-1} at 0.5 mM and 4900 M^{-1} at 8 mM (Table S1 in the SI). Exchange spectroscopy (EXSY) NMR experiments on a 2.4 mM solution at 293 K allowed the rate constants for double helix formation and dissociation to be calculated as 107 s^{-1} M^{-1} and 0.061 s^{-1}, respectively. The double-helical dimer was also characterized in the solid state by X-ray crystallography (see the SI). These results further expand the already wide range of aromatic amino acids that are compatible with double helix formation to include the central **pyr−pyz−pyr** segment. Double helices do not form in the case of the capsule sequence **1** from which **2** is derived.[4] This is explained by the poor ability of the terminal quinoline units to undergo the springlike extension required for double helix formation.[9] Suppressing (or reducing the number of) quinoline units that code for a narrow helix diameter has been observed to promote double helix formation in other systems.[10]

Host−guest interactions were then investigated using both ^{1}H NMR and circular dichroism (CD) spectroscopy to estimate the ability of **2** to fold around tartaric acid derivative **3**. Upon the addition of **3** to a 0.1 mM solution of **2** in $CDCl_3$, a concentration at which the single-helical conformation of **2** predominates (>99%) (Figure 2A, open circles), the NMR

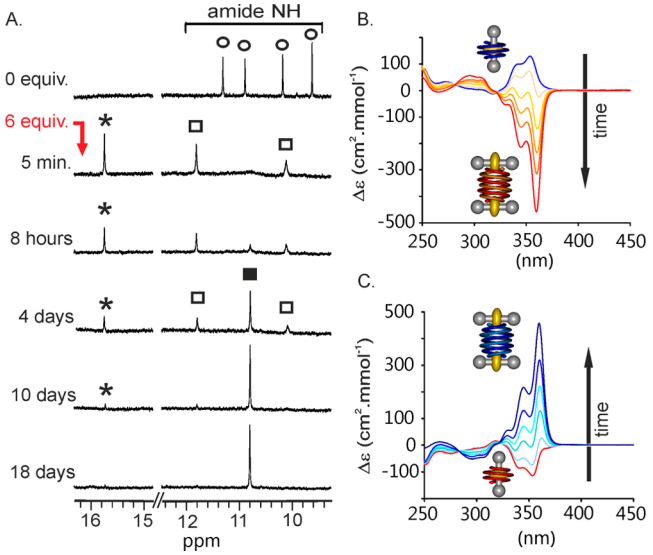

Figure 2. (A) Parts of the 300 MHz ^{1}H NMR spectra of **2** (0.1 mM) in $CDCl_3$ at 298 K (top to bottom) before the addition of guest and 5 min, 8 h, 4 days, 10 days, and 18 days after the addition of 6 equiv of **3**. Open circles denote signals of the empty capsule. The asterisks denote the hydrogen-bonded acid protons of the guest in **2**⊃**3**. The N*H* amide signals of the single-helical host−guest complex are marked with open squares, whereas those of the double-helical host−guest complex are marked with a solid square. (B) CD spectra of **2** (0.1 mM in $CDCl_3$) at 298 K 10 min after the addition of 6 equiv of **3**-(D) (blue spectrum) and after 5 h, 15 h, 30 h, 70 h, and 18 days (increasing red intensity). (C) CD spectra of **2** (0.1 mM in $CDCl_3$) 10 min after the addition of 6 equiv of **3**-(L) (red spectrum) and after 5 h, 15 h, 30 h, 70 h, and 18 days (increasing blue intensity).

signals of the latter disappeared, and signals due to a new complex in which **3** is bound within the cavity of **2** emerged (Figure 2A, open squares). The binding constant was measured accurately through the integral ratios of the free and bound receptor amide resonances to be $K_a = 2.7 \times 10^4$ L mol^{-1} at 298 K in $CDCl_3$. On the basis of previous investigations of the binding of tartaric acid to **1**,[4] the sharp signal at 15.7 ppm in the spectrum of **2**⊃**3** was assigned to the acid protons of the guest, which are hydrogen-bonded to the central **N** units of **2**, suggesting similar modes of binding of tartaric acid by **1** and **2**. This similarity was further expressed in CD titrations, for which strong responses with opposite signs appeared upon the addition of **3**-(D) or **3**-(L).

dx.doi.org/10.1021/ja3064364 | *J. Am. Chem. Soc.* XXXX, XXX, XXX−XXX

The host−guest interaction is fully diastereoselective and results in an induced handedness in **2**. The strong negative Cotton effect at 360 nm for **2**⊃**3**-(L) (Figure 2C, red spectrum) suggests that the same handedness preference occurs in **2**⊃**3** as in **1**⊃tartaric acid: the L enantiomer favors *M* helicity. CD was also employed as an additional technique to support the NMR titrations. The progressive addition of **3**-(D) into a 10 μM solution of **2** resulted in the appearance a positive signal that gave an excellent fit to a 1:1 binding model.[11] The binding constant measured by CD at 273 K (4.4×10^4 L mol^{-1}) was reasonably close to that obtained by NMR analysis at 298 K. These results, along with the detailed structural data available for the **1**⊃tartaric acid complex,[4a] allowed the proposal of an energy-minimized model of the structure of (*M*)-**2**⊃**3**-(L) having the expected foldaxane architecture with the helix wrapped around the dumbbell guest (Figure 3A,B) and the carboxylic acid groups of the guest hydrogen-bonded to the **N** units of the host.

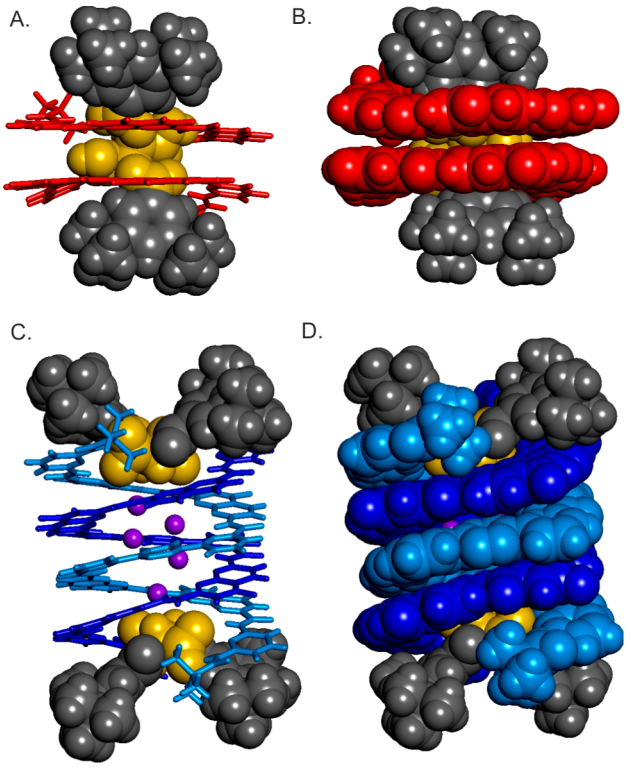

Figure 3. (A) CPK (guest) and tube (host) and (B) CPK (host and guest) representations of the structure of the foldaxane (*M*)-**2**⊃**3**-(L) as obtained by molecular modeling using Maestro version 6.5 with the Merck molecular force field. (C) CPK (guest) and tube (host) and (D) CPK (host and guest) representations of the solid-state structure of $[(P)\text{-}\mathbf{2}]_2$⊃[**3**-(L)]$_2$. The isobutyl side chains and solvent molecules have been omitted for clarity, except for the water cluster included in the cavity of the double helix (purple balls).

The kinetics of the quantitative formation of **2**⊃**3** from the single helix of **2** and the kinetics of guest-induced single-helix handedness inversion are fast: a steady state was reached within seconds (before CD or NMR measurements can be carried out).[6a,b,12] When stored at −18 °C, a sample remained unchanged for weeks. However, upon standing at 25 °C, the complex **2**⊃**3** slowly disappeared over the course of days and was quantitatively replaced by another species, showing that **2**⊃**3** is not the thermodynamic product. This conversion was monitored by both NMR spectroscopy, where all of the initial signals, including the guest resonance at 15.7 ppm, disappeared (Figure 2A), and by CD spectroscopy, where a remarkable inversion of sign at 360 nm was observed. This modification reflects an inversion of the handedness[13] of **2** mediated by the guest that changes the helicity from *P* to *M* in the case of **3**-(D) and from *M* to *P* in the case of **3**-(L) (Figure 2B,C).

X-ray-quality single crystals were obtained by slow diffusion of hexane into a chloroform solution of **2** mixed with racemic **3** at thermodynamic equilibrium, and the solid-state structure was solved (Figure 3C,D). It revealed an original architecture completely different from that of the foldaxane **2**⊃**3** composed of a 2:2 complex consisting of $(\mathbf{2})_2$ as a double helix with a bound molecule of **3** capping the helix cavity at each extremity. The structure of $(\mathbf{2})_2$ complexed with **3** much resembles its structure without bound **3**. As a slight difference, the duplex diameter is slightly decreased in the complex with **3**, as reflected by a helix span longer by about half a pyridine ring. In the crystal structure, **3**-(L) is bound to $[(P)\text{-}\mathbf{2}]_2$ and **3**-(D) is bound to $[(M)\text{-}\mathbf{2}]_2$, consistent with the inversion of preferred handedness observed over time when **2** was titrated with either **3**-(L) or **3**-(D) (Figure 2). Each tartaric acid derivative adopts a typical conformation with trans acid groups and gauche hydroxy groups. The carboxylic acid groups are oriented perpendicular to the edge of the helical strand and doubly hydrogen-bonded to the distal pyridines ($d_{OH\cdots N}$ = 2.63 Å, $d_{NH\cdots OC}$ = 2.99 Å), giving a total of eight intermolecular hydrogen bonds. The interactions between **3** and $(\mathbf{2})_2$ differ from those between **3** and single-helical **2** in that the hydrogen bonds occur with the **N** units of **2** and the pyridine units of $(\mathbf{2})_2$. Also, van der Waals contacts between the 3,5-di-*tert*-butylphenyl rings of **3** and **2** appear to be more extensive in the crystal structure of $(\mathbf{2})_2$⊃$(\mathbf{3})_2$ than in the calculated structure of **2**⊃**3**. However, it is unclear why these differences result in the much higher stability of $(\mathbf{2})_2$⊃$(\mathbf{3})_2$.

Consistent with the solid-state structure, evidence of the double helical nature of the host in solution was found. In particular, the ^{1}H signals of **2** in $(\mathbf{2})_2$⊃$(\mathbf{3})_2$ are strongly upfield-shifted from those of **2** in **2**⊃**3** as a result of enhanced ring current effects in the double-helical dimer.[8] A ^{1}H DOSY experiment confirmed the larger size of $(\mathbf{2})_2$⊃$(\mathbf{3})_2$ relative to **2**⊃**3** (Figure S4). Adding racemic **3** to a racemic (*P*/*M*) solution of $(\mathbf{2})_2$ (at 30 mM, the double helix prevails) readily caused shifts of both the aromatic and amide signals, reflecting the fact that $[(P/M)\text{-}\mathbf{2}]_2$ and its complexes with **3**-(L) and **3**-(D) exchange rapidly on the NMR time scale (Figure S12). The association constant of $(\mathbf{2})_2$ and **3** was too large to be calculated accurately from curve fitting of the titration data. Indeed, this binding constant is expected to be significantly larger than that for binding of **3** to single-helical **2** (i.e., larger than 2.7×10^4 L mol^{-1}), as the apparent dimerization of **2** to form $(\mathbf{2})_2$ is strongly enhanced in the presence of **3** (Figure 2). Also, this titration experiment did not allow any cooperativity between the binding of the first and second guests to be characterized.

In an other titration, a single enantiomer of **3** was added to a racemic (*P*/*M*) solution of $(\mathbf{2})_2$ (Figure S14). This resulted in the induction of CD bands and splitting of ^{1}H NMR signals into two sets, one having chemical shift values identical to those observed in the titration with racemic **3** and one having chemical shift values almost identical to those of free $(\mathbf{2})_2$ (see the SI). This reflects the fact that the pure enantiomer of **3** forms a stable complex with the $(\mathbf{2})_2$ duplex that has the matching stereochemistry and a weak complex or no complex

dx.doi.org/10.1021/ja3064364 | *J. Am. Chem. Soc.* XXXX, XXX, XXX−XXX

at all with the $(\mathbf{2})_2$ duplex having the mismatching stereochemistry, suggesting that the interaction between $(\mathbf{2})_2$ and **3** is also strongly diastereoselective. Since the equilibrium between $[(P)\text{-}\mathbf{2}]_2$ and $[(M)\text{-}\mathbf{2}]_2$ is slow on the NMR time scale, **3** acts as a sort of chiral shift reagent that resolves them into distinct signals before their interconversion occurs.

Interestingly, the induced CD spectrum of **2** resulting from a handedness bias by **3** was found to be ∼5 times more intense in $(\mathbf{2})_2\supset(\mathbf{3})_2$ than in **2**⊃**3** (Figure 2B,C) despite the fact that handedness induction is (close to) quantitative in both cases. The $\Delta\varepsilon$ values appear to be higher for double-helical $(\mathbf{2})_2$ than for single-helical **2**, whose helix pitch is half as small.

In summary, guest **3** enhances the thermodynamic stability of the double-helical duplex $(\mathbf{2})_2$ but simultaneously reduces the kinetics of $(\mathbf{2})_2$ production upon forming a foldaxane with monomeric **2**, which can be long-lived at low temperature. While each individual equilibrium appears to be relatively fast when assessed in the millimolar range, the formation of **2**⊃**3** at 0.1 mM results in a very low concentration of single-helical **2**, which slows the formation of $(\mathbf{2})_2$. Similarly, the formation of $(\mathbf{2})_2\supset(\mathbf{3})_2$ is slower when the concentrations of both $(\mathbf{2})_2$ and free **3** are low. The sequence of steps for conversion of **2**⊃**3** into $(\mathbf{2})_2\supset(\mathbf{3})_2$ is shown in Figure 1: (*i*) dissociation into **2** and **3**; (*ii*) inversion of the helix handedness of **2** (see ref 14 for a possible mechanism); (*iii*) association of **2** into $(\mathbf{2})_2$; and (*iv*) binding of **3** to $(\mathbf{2})_2$. The time scales involved in the equilibria at each step allow the isolation of both the kinetic and thermodynamic supramolecular products and monitoring of the inversion of chiroptical properties with time as the system first evolves toward a product with one handedness and then reverts into another product having the opposite handedness.

■ ASSOCIATED CONTENT

Supporting Information

Experimental details for synthetic procedures, spectroscopic data, and CIFs for $(\mathbf{2})_2$ and $(\mathbf{2})_2\supset(\mathbf{3})_2$. This material is available free of charge via the Internet at http://pubs.acs.org.

■ AUTHOR INFORMATION

Corresponding Author

i.huc@iecb.u-bordeaux.fr

Notes

The authors declare no competing financial interest.

■ ACKNOWLEDGMENTS

This work was supported by the Conseil Régional d'Aquitaine (predoctoral fellowship to Q.G.) and by ANR (Grant ANR-09-BLAN-0082-01). We thank Ms. Axelle Grélard for her assistance with NMR measurements.

■ REFERENCES

(1) (a) Mathias, J. P.; Simanek, E. E.; Seto, C. T.; Whitesides, G. M. *Angew. Chem., Int. Ed. Engl.* **1993**, *32*, 1766. (b) Paraschiv, V.; Crego-Calama, V.; Ishi-i, T.; Padberg, C. J.; Timmerman, P.; Reinhoudt, D. N. *J. Am. Chem. Soc.* **2002**, *124*, 7638. (c) Korevaar, P. A.; George, S. J.; Markvoort, A. J.; Smulders, M. M. J.; Hilbers, P. A. J.; Schenning, A. P. H. J.; De Greef, T. F. A.; Meijer, E. W. *Nature* **2012**, *481*, 492.

(2) (a) Hasenknopf, B.; Lehn, J.-M.; Boumediene, N.; Dupont-Gervais, A.; Van Dorsselaer, A.; Kneisel, B.; Fenske, D. *J. Am. Chem. Soc.* **1997**, *119*, 10956. (b) Hasenknopf, B.; Lehn, J.-M.; Boumediene, N.; Leize, E.; Van Dorsselaer, A. *Angew. Chem., Int. Ed.* **1998**, *37*, 3265. (c) Levin, M. D.; Stang, P. J. *J. Am. Chem. Soc.* **2000**, *122*, 7428. (d) Cangelosi, V. M.; Carter, T. G.; Zakharov, L. N.; Johnson, D. W. *Chem. Commun.* **2009**, 5606.

(3) (a) Kinbara, K.; Aida, T. *Chem. Rev.* **2005**, *105*, 1377. (b) Gan, Q.; Ferrand, Y.; Bao, C.; Kauffmann, B.; Grélard, A.; Jiang, H.; Huc, I. *Science* **2011**, *331*, 1172.

(4) (a) Ferrand, Y.; Kendhale, A. M.; Kauffmann, B.; Grélard, A.; Marie, C.; Blot, V.; Pipelier, M.; Dubreuil, D.; Huc, I. *J. Am. Chem. Soc.* **2010**, *132*, 7858. (b) Ferrand, Y.; Nagula, C.; Kendhale, A. M.; Aube, C.; Kauffmann, B.; Grélard, A.; Laguerre, M.; Dubreuil, D.; Huc, I. *J. Am. Chem. Soc.* **2012**, *134*, 11282.

(5) Ferrand, Y.; Gan, Q.; Kauffmann, B.; Jiang, H.; Huc, I. *Angew. Chem., Int. Ed.* **2011**, *50*, 7572.

(6) (a) Nishinaga, T.; Tanatani, A.; Oh, K.; Moore, J. S. *J. Am. Chem. Soc.* **2002**, *124*, 5934. (b) Tanatani, A.; Hughes, T. S.; Moore, J. S. *Angew. Chem., Int. Ed.* **2002**, *41*, 325. (c) Petitjean, A.; Cuccia, L. A.; Schmutz, M.; Lehn, J. M. *J. Org. Chem.* **2008**, *73*, 2481.

(7) Sugiura, M.; Tokudomi, M.; Nakajima, M. *Chem. Commun.* **2010**, *46*, 7799.

(8) (a) Berl, V.; Huc, I.; Khoury, R.; Krische, M. J.; Lehn, J.-M. *Nature* **2000**, *407*, 720. (b) Gan, Q.; Bao, C.; Kauffmann, B.; Grélard, A.; Xiang, J.; Liu, S.; Huc, I.; Jiang, H. *Angew. Chem., Int. Ed.* **2008**, *47*, 1715. (c) Baptiste, B.; Zhu, J.; Haldar, D.; Kauffmann, B.; Léger, J.-M.; Huc, I. *Chem.—Asian J.* **2010**, *5*, 1364.

(9) Jiang, H.; Léger, J.-M.; Huc, I. *J. Am. Chem. Soc.* **2003**, *125*, 3448.

(10) (a) Berni, E.; Kauffmann, B.; Bao, C.; Lefeuvre, J.; Bassani, D. M.; Huc, I. *Chem.—Eur. J.* **2007**, *13*, 8463. (b) Berni, E.; Garric, J.; Lamit, C.; Kauffmann, B.; Léger, J.-M.; Huc, I. *Chem. Commun.* **2008**, 1968.

(11) Association constants (K_a) were obtained using the WINEQNMR software. See: Hynes, M. J. *J. Chem. Soc., Dalton Trans.* **1993**, 311.

(12) (a) Hou, J.-L.; Shao, X.-B.; Chen, G.-J.; Zhou, Y.-X.; Jiang, X.-K.; Li, Z.-T. *J. Am. Chem. Soc.* **2004**, *126*, 12386. (b) Maurizot, V.; Dolain, C.; Huc, I. *Eur. J. Org. Chem.* **2005**, 1293. (c) Goto, H.; Furusho, Y.; Yashima, E. *J. Am. Chem. Soc.* **2007**, *129*, 9168. (d) Waki, M.; Abe, H.; Inouye, M. *Angew. Chem., Int. Ed.* **2007**, *46*, 3059.

(13) For examples of handedness inversion, see: (a) Fujiki, M. *J. Am. Chem. Soc.* **2000**, *122*, 3336. (b) Sakurai, S.-i.; Okoshi, K.; Kumaki, J.; Yashima, E. *J. Am. Chem. Soc.* **2006**, *128*, 5650. (c) Okoshi, K.; Sakurai, S.-i.; Ohsawa, S.; Kumaki, J.; Yashima, E. *Angew. Chem., Int. Ed.* **2006**, *45*, 8173. (d) Johnson, R. S.; Yamazaki, T.; Kovalenko, A.; Fenniri, H. *J. Am. Chem. Soc.* **2007**, *129*, 5735. (e) Meudtner, R. M.; Hecht, S. *Angew. Chem., Int. Ed.* **2008**, *47*, 4926. (f) Peterca, M.; Imam, M. R.; Ahn, C.-H.; Balagurusamy, V. S. K.; Wilson, D. A.; Rosen, B. M.; Percec, V. *J. Am. Chem. Soc.* **2011**, *133*, 2311. (g) Akine, S.; Hotate, S.; Nabeshima, T. *J. Am. Chem. Soc.* **2011**, *133*, 13868.

(14) Delsuc, N.; Kawanami, T.; Lefeuvre, J.; Shundo, A.; Ihara, H.; Takafuji, M.; Huc, I. *ChemPhysChem* **2008**, *9*, 1882.